Analytical Study for Wave Propagation over a Turbulent-Trapezoidal Breakwater

Ikha Magdalena, Hany Qoshirotur Rif'atin, and Dominic Edmund Reeve

***Abstract*—In this paper, a mathematical model is formulated to investigate the effect of a submerged trapezoidal breakwater and its turbulence on reducing wave transmission. The breakwater has a composite slope on the side facing the incident waves, in common with many practical examples. Wave motions obeying modified Linear Shallow Water Equations (LSWE) are considered with the addition of a diffusion term in the momentum equation to represent the energy dissipation due to turbulent motion promoted by the breakwater. The modified equations are solved analytically using the Separation of Variables Method to obtain wave reflection and transmission coefficients. Test cases are presented to validate the analytical solutions against the known solutions for common breakwater structures, such as rectangular breakwaters. For the composite-sloped structure, wave shoaling may occur, increasing the incident wave amplitude. After passing over the breakwater, the wave amplitude decreases as it propagates into deeper water. Here, the diffusion effect caused by the breakwater works as a reducer to help reduce the wave amplitude. Applying the model to the real bathymetry of the coast of Aceh, Sumatera, Indonesia, shows that the breakwater can reduce the tsunami wave amplitude slightly. It also shows that the diffusion coefficient reduces the wave amplitude differently depending on the characteristics of the wave itself.**

***Index Terms*—diffusion term, shallow water equation, submerged trapezoidal breakwater, transmission coefficient, turbulence.**

I. Introduction

WAVE height changes as they move closer to the coast for a variety of reasons, including refraction, diffraction, reflection, wave breaking, wave-current interaction, friction, wind-induced wave growth, and wave shoaling. The phenomenon of wave shoaling occurs when surface waves enter shallower water and increase in height. It is due to the fact that group velocity diminishes as water depth decreases. To maintain a constant energy flow, the decline in group velocity must be compensated for by a rise in wave height [1]. In the absence of the other wave effects, shoaling arises purely as a result of variations in mean water depth – without concern for changes in wave propagation direction or dissipation. Additionally, it is shown in [2] that the behaviour of wave shoaling is dependent on the cross-sectional shape of the seabed on which the wave propagates. As the wave propagates, shoaling will continue until the wave becomes unstable and begins to break, dissipating energy. Shoaling is one of the reasons that long waves, such as tsunamis, storm surges, and swells, cause significant disruption to coastal areas. Since such waves have very long wavelengths in the deep ocean and contain huge amounts of water in each wavelength, they will shoal as high as they do as the water gets shallower. And as the waves become higher, their energy, which is mainly in the form of kinetic energy, is transformed into potential energy, creating a devastating impact on the coast. Several researchers have investigated the phenomenon of wave shoaling on infinite steps [3], [4] and over a shelf with a linear transition [2], [5]–[7].

Recognizing the consequences of wave shoaling, researchers and engineers in relevant fields have been attempting to propose a variety of strategies to protect the coastal environment. One of the proposals that has gained the most attention in recent years is the breakwater, a structure developed to defend the shoreline from wave action, especially by reducing the wave height that was previously amplified due to shoaling. Breakwaters may be emergent, with their crests still visible above the still water surface or submerged. Emergent breakwaters act as an obstacle to wave propagation, causing the wave reflection phenomenon and potentially wave breaking. Submerged breakwaters induce partial reflection, allowing some wave energy to be transmitted to the shore. This is appropriate in circumstances where some wave actions are tolerable. The cross-sectional geometry of submerged breakwaters will affect the wave transmission and reflection, making it a critical design factor of the structure.

Over the years, many studies have investigated the impacts of submerged breakwaters on wave height reduction. Early research on the effect of rectangular breakwaters on reducing wave height can be traced back to [8]–[10]. Other researchers followed in their steps by evaluating the same subject using different models and methods [11], [12]. Recently, Magdalena et al. [13] extended these studies to analyse the wave transmitted amplitude as it travels over multiple rectangular breakwaters using linear shallow water equations. Furthermore, several researchers went above and beyond to investigate the effects of porous, floating, or flexible structures [14]–[20]. Dalrymple and Kirby [21], on the other hand, totally altered the shape of the breakwater into ripples rather than merely modifying its characteristics and observed its effect on wave height reduction using Green's Theorem. Furthermore, Lin [22], Chang and Liou [23], and Behera and Khan [24] generalised the form of the submerged breakwater by making it trapezoidal and studying the structure using a variety of models such as linear shallow water equations, Potential Theory, and Helmholtz Equation. However, neither of those studies considered the turbulence effect, which is ideally present alongside the breakwater structure. This effect is an important feature of breakwater

Manuscript received July 14, 2021; revised Dec 28, 2021. This work was supported by Bandung Institute of Technology (ITB) research fund.

Ikha Magdalena is a Lecturer and researcher in Faculty of Mathematics and Natural Sciences, Bandung Institute of Technology, Indonesia (corresponding author; e-mail: ikha.magdalena@math.itb.ac.id).

Hany Qoshirotur Rif'atin is a research assistant in the Faculty of Mathematics and Natural Sciences, Bandung Institute of Technology, Indonesia (e-mail: hany.qoshirotur@gmail.com).

Dominic Edmund Reeve is a Professor of Coastal Engineering and Head of the Zienkiewicz Centre for Computational Engineering in Swansea University, UK (e-mail: d.e.reeve@swansea.ac.uk).

performance since it is an effective wave energy dissipator. Wave energy may decrease drastically near the breakwater owing to increased turbulent dissipation and energy loss from lower harmonics to higher harmonics [25]. As a result, several experiments were carried out in order to capture the turbulence effect induced by the breakwater so that the structure's effect on decreasing wave height could be properly studied. Experiments were carried out to assess the effect of rectangular breakwaters on wave amplitude suppression [26]–[30]. Further, Beji and Bettjes [31] and Ohyama et al. [32] conducted experiments to investigate the interaction of waves and trapezoidal breakwaters. Extending on those reports, Garcia et al. [33] and Kramer et al. [34] performed experiments on the composite-sloped trapezoidal breakwater. Such experimental findings are highly likely to be accurate. However, laboratory tests are quite costly due to the inflexibility of this approach, which must be modified every time we want to observe other set-ups or use different parameter values.

Thus, in this paper, we will propose a model to investigate the effectiveness of submerged breakwater structures in reducing wave height while considering the turbulence effect on the breakwater. We will concentrate on the more general form of breakwater, the composite-trapezoidal shape, such that the findings of this paper can be applied to simpler scenarios, such as trapezoidal and rectangular structures. The model suggested here is the Linear Shallow Water Equations (LSWE), which will be modified by incorporating a diffusion term into the momentum equation to represent the turbulence effect induced by the breakwater. The wave transmission and reflection coefficients will then be determined analytically using this model. These analytical solutions can be a significant development to the study of breakwater, especially when a turbulence is involved, since we can hardly find the exact solutions from previous researches. These two coefficients, especially the transmission coefficient, are critical in assessing how much the breakwater has reduced the wave height, and thus how effective the breakwater structure is in reducing the wave amplitude. Using this model, we can easily adjust the model's setup without spending a lot of money. Besides that, as opposed to other models such as Navier-Stokes Equations, Boussines-type Model, Green's Theorem, or Potential Theory, the LSWE are simpler to solve analytically, which can save the cost of derivation of analytical solutions. However, to validate this model, we must equate its accuracy to that of previous models. Therefore, we can compare the analytical solutions obtained using LSWE to solutions for simplified cases, such as rectangular breakwaters [10] and wave shoaling solution [3]. Following that, the validated model and analytical solutions will be used to investigate the influence of diffusion and breakwater geometry on wave transmission. In addition, the model will be used to examine the effect of a composite-sloped trapezoidal submerged breakwater on the actual bathymetry of the coast of Aceh, Sumatera, Indonesia.

To achieve our objectives, we will present the paper in five sections, the first of which will explain the problem and the goals of this paper. In the second section, the governing equations will be briefly explained. The third section provides the analytical solutions for the wave communication and reflection coefficients, which serve as measurement tools for the efficacy of the breakwater. Section 4 contains the test cases that will be used to validate our model, which will then be used to investigate the behaviour of wave transmission because of breakwater structure and diffusion coefficient variations, as well as the interaction of waves and composite-sloped trapezoidal breakwater over real bathymetry in Aceh. Finally, the paper will be concluded with Section 5.

II. Mathematical Model

In this section, we formulate a 1-D time-dependent mathematical model of wave propagation over a composite-sloped submerged trapezoidal breakwater. The model that we use is based on Linear Shallow Water Equations (LSWE). Here, the modification of LSWE is needed to include the effect of turbulent motions that are enhanced by the breakwater. The effect of turbulence on the momentum balance can be represented by $\nu_t \nabla(\nabla.u)$ where ν_t is the eddy viscosity [35]. Eddy viscosity is usually taken to be uniform in space [36]–[38]. Assuming that ν_t is a constant, we can rewrite the turbulence term $\nu_t \nabla(\nabla.u)$ as a simpler diffusion term $\kappa \frac{\partial^2 u}{\partial x^2}$, with $\kappa = \nu_t$ denotes the uniform diffusion coefficient. Here, we use the diffusion term to model energy dissipation in the vicinity of the breakwater, so we will specify κ to be piecewise constant within sub-domains of the main domain. Thus, our governing equations will be

$$\eta_t + (hu)_x = 0, \tag{1}$$

$$u_t + g\eta_x = 0, \tag{2}$$

where (1) is the mass conservation equation and (2) is the momentum conservation equation. Notation η denotes the wave elevation that is measured from the still water level as depicted in Fig. 1, u denotes the horizontal wave velocity, g is the gravity acceleration, and h denotes the water depth calculated from undisturbed water position. Using the Separation of Variables Method, we rewrite the wave elevation and velocity as $\eta(x,t) = \overline{\eta}(x)\, e^{-i\omega t}$ and $u(x,t) = \overline{u}(x)\, e^{-i\omega t}$ respectively. For ease of reference, we will use the following notation from now on: $\frac{d\overline{\eta}(x)}{dx} = \overline{\eta}_x$ and $\frac{d^2\overline{\eta}(x)}{dx^2} = \overline{\eta}_{xx}$, and similarly for other dependent and independent variables.

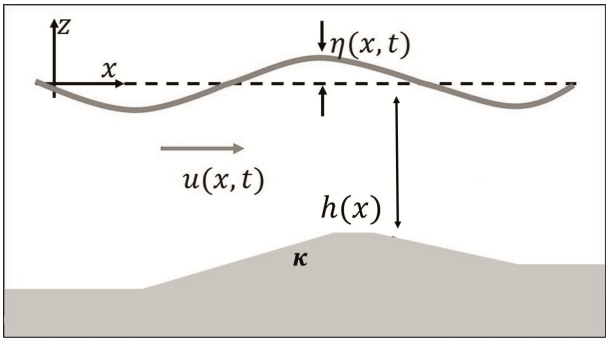

Fig. 1: Illustration of modified Linear Shallow Water Equation

Substituting η and u to (1) and (2) produces the following equation

$$\omega^2 \overline{u}(x) + 2gh_x \overline{u}_x + (gh(x) - i\omega\kappa)\, \overline{u}_{xx} = 0, \tag{3}$$

and relation

$$\overline{\eta}\,(x) = \frac{1}{i\omega}(h\overline{u})_x, \tag{4}$$

where ω denotes the wave angular frequency and $h(x)$ is the undisturbed water depth.

Considering a composite-sloped submerged trapezoidal breakwater which set-up is illustrated in Fig. 2, we split the depth $h(x)$ into six domains, on which we can write as

$$h(x) = \begin{cases} h_0 & ,x \le x_0 \\ h_0 + \frac{h_1-h_0}{x_1-x_0}(x-x_0) & ,x_0 < x \le x_1 \\ h_1 + \frac{h_2-h_1}{x_2-x_1}(x-x_1) & ,x_1 < x \le x_2 \\ h_2 & ,x_2 < x \le x_3 \\ h_2 + \frac{h_3-h_2}{x_4-x_3}(x-x_3) & ,x_3 < x \le x_4 \\ h_3 & ,x > x_4. \end{cases} \tag{5}$$

Next, the general solution of $\overline{\eta}$ and $\overline{u}$ will be calculated for each domain using the bottom elevation described by (5) and the dynamic governing equations (3) and (4).

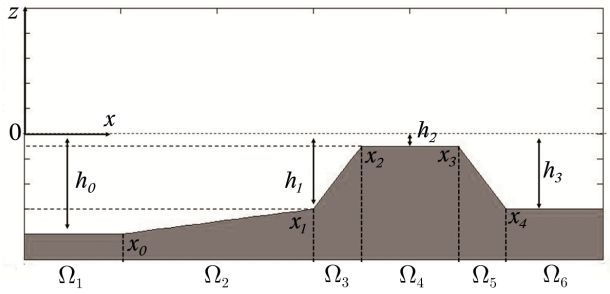

Fig. 2: Set-up of the breakwater structure

III. Analytical Solution

The analytical solution described in this section is in the form of a reflection and transmission coefficient, which is the ratio of reflected or transmitted amplitude to the incoming wave amplitude. The coefficients are calculated using the general solution of $\overline{\eta}$ and $\overline{u}$ for each domain, which can be obtained by solving (3) and (4). The general solution is then solved using matching conditions and elimination procedures to find the reflected and transmission coefficients.

A. General Solution of η and u

1) Flat Domain Ω_1, Ω_4 and Ω_6: For domain Ω_1, we consider $h(x) = h_0$ as the depth of the water. We substitute $h(x)$ into (3) and (4) to find the following equations

$$\begin{aligned} \overline{\eta}_x &= \tfrac{h_0}{i\omega}\overline{u}_{xx}, \\ \omega^2\overline{u} + (gh - i\omega\kappa)\,\overline{u}_{xx} &= 0. \end{aligned} \tag{6}$$

Because the turbulence effects are considered to be limited to the region of the breakwater, we assume that there will be no diffusion in either of the domains Ω_1 and Ω_6. Consequently, the value of κ is set as zero in the domain Ω_1, so that the last equation becomes

$$\omega^2\overline{u} + gh\overline{u}_{xx} = 0. \tag{7}$$

which give solution for $\overline{\eta}$ and $\overline{u}$ that can be written as follows.

$$\overline{u}\,(x) = \frac{gk_0}{\omega}(A_I e^{ik_0x} - A_r e^{-ik_0x}), \tag{8}$$

$$\overline{\eta}\,(x) = A_I e^{ik_0x} + A_r e^{-ik_0x}, \tag{9}$$

with A_I is the amplitude of the incoming wave, A_r is the reflected wave amplitude, and $k_0 = \omega/\sqrt{gh_0}$ is the wave number in domain Ω_1. The same assumption is used for the domain Ω_6, so that $\kappa = 0$. With depth $h\,(x) = h_3$, the solution of $\overline{\eta}$ and $\overline{u}$ in domain Ω_6 are

$$\overline{u}\,(x) = \frac{gk_3}{\omega}A_t e^{ik_3x}, \tag{10}$$

$$\overline{\eta}\,(x) = A_t e^{ik_3x}, \tag{11}$$

in which A_t is the transmitted wave amplitude and $k_3 = \omega/\sqrt{gh_3}$. It has been assumed that waves propagate freely out of the right-hand side of Ω_6 without any reflection.

In domain Ω_4 with water depth $h\,(x) = h_2$, the assumption of zero diffusion is not applicable because the domain is part of the breakwater structure. Consequently, the solutions of $\overline{\eta}$ and $\overline{u}$ obtained for this domain are

$$\overline{u}\,(x) = \left(\frac{gk_2}{\omega} - \frac{i\kappa k_2}{h_2}\right)(A_5 e^{ik_2x} - A_6 e^{-ik_2x}), \tag{12}$$

$$\overline{\eta}(x) = A_5 e^{ik_2x} + A_6 e^{-ik_2x}, \tag{13}$$

where A_5 and A_6 are unknown constants, and $k_2 = \omega/\sqrt{gh_2 - i\omega\kappa}$.

2) Sloping Domain Ω_2, Ω_3 and Ω_5: For domain Ω_2, the water depth is $h(x) = h_0 + \frac{h_1-h_0}{x_1-x_0}(x-x_0)$, so that (3) becomes

$$\begin{aligned} &\omega^2\overline{u} + \tfrac{2g(h_1-h_0)}{x_1-x_0}\overline{u}_x \\ &+ \left(gh_0 + \tfrac{g(h_1-h_0)}{x_1-x_0}(x-x_0) - i\omega\kappa\right)\overline{u}_{xx} \quad = 0, \end{aligned} \tag{14}$$

which can be rewritten as

$$\frac{(x+\tilde{x}_0)}{2}\overline{u}_{xx} + \overline{u}_x + \frac{\omega^2}{2g}\tilde{x}_1\overline{u} = 0, \tag{15}$$

where $\tilde{x}_0 = \frac{x_1h_0 - x_0h_1}{h_1-h_0} - \frac{i\omega\kappa(x_1-x_0)}{g(h_1-h_0)}$ and $\tilde{x}_1 = (x_1 - x_0)/(h_1-h_0)$. The solution of (15) is

$$\overline{u}(x) = \frac{1}{\sqrt{x+\tilde{x}_0}}(A_1J_1(\alpha_0(x)) + A_2Y_1(\alpha_0(x)), \tag{16}$$

in which $J_1(x)$ and $Y_1(x)$ are Bessel function of the first kind and the second kind, respectively, while $\alpha_0(x) = \frac{2\omega}{\sqrt{g}}\sqrt{\tilde{x}_1}\sqrt{x+\tilde{x}_0}$. A_1 and A_2 are unknown constants. Then, substituting the solution of $\overline{u}$ that we have obtained into (4) we will get the solution of $\overline{\eta}$ as follows.

$$\begin{aligned}\overline{\eta}(x) = \; & \tfrac{1}{i\omega(x+\tilde{x}_0)^{\frac{3}{2}}}\left(A_1\left(-\tfrac{i\omega\kappa}{g}J_1(\alpha_0(x))\right.\right.\\ & +\tfrac{\alpha_0(x)(x_1h_0-x_0h_1+xh_1-xh_0)}{2(x_1-x_0)}J_0(\alpha_0(x))\Big)\\ & +A_2\left(-\tfrac{i\omega\kappa}{g}Y_1(\alpha_0(x))\right.\\ & \left.\left.+\tfrac{\alpha_0(x)(x_1h_0-x_0h_1+xh_1-xh_0)}{2(x_1-x_0)}Y_0(\alpha_0(x))\right)\right).\end{aligned} \tag{17}$$

Using the same method as before, for domain Ω_3 with $h(x) = h_1 + \frac{h_2-h_1}{x_2-x_1}(x-x_1)$ and domain Ω_5 with $h(x) = h_2 + \frac{h_3-h_2}{x_4-x_3}(x-x_3)$, the analytical solutions of $\overline{u}$ and $\overline{\eta}$, respectively, are

$$\begin{aligned}\overline{u}(x) = \; & \tfrac{1}{\sqrt{x+\tilde{x}_2}}(A_3J_1(\alpha_1(x)) + A_4Y_1(\alpha_1(x)),\\ \overline{\eta}(x) = \; & \tfrac{1}{i\omega(x+\tilde{x}_3)^{\frac{3}{2}}}\left(A_3\left(-\tfrac{i\omega\kappa}{g}J_1(\alpha_1(x))\right.\right.\\ & +\tfrac{\alpha_1(x)(x_2h_1-x_1h_2+xh_2-xh_1)}{2(x_2-x_1)}J_0(\alpha_1(x))\Big)\\ & +A_4\left(-\tfrac{i\omega\kappa}{g}Y_1(\alpha_1(x))\right.\\ & \left.\left.+\tfrac{\alpha_1(x)(x_2h_1-x_1h_2+xh_2-xh_1)}{2(x_2-x_1)}Y_0(\alpha_1(x))\right)\right),\end{aligned} \tag{18}$$

and

$$\begin{aligned}\overline{u}(x) = \; & \tfrac{1}{\sqrt{x+\tilde{x}_4}}(A_7J_1(\alpha_2(x)) + A_8Y_1(\alpha_2(x)),\\ \overline{\eta}(x) = \; & \tfrac{1}{i\omega(x+\tilde{x}_4)^{\frac{3}{2}}}\left(A_7\left(-\tfrac{i\omega\kappa}{g}J_1(\alpha_2(x))\right.\right.\\ & +\tfrac{\alpha_2(x)(x_4h_2-x_3h_3+xh_3-xh_2)}{2(x_4-x_3)}J_0(\alpha_2(x))\Big)\\ & +A_8\left(-\tfrac{i\omega\kappa}{g}Y_1(\alpha_2(x))\right.\\ & \left.\left.+\tfrac{\alpha_2(x)(x_4h_2-x_3h_3+xh_3-xh_2)}{2(x_4-x_3)}Y_0(\alpha_2(x))\right)\right),\end{aligned} \tag{19}$$

in which A_3, A_4, A_7, and A_8 denote the unknown constants, whereas

$$\begin{aligned}&\tilde{x}_2 = \tfrac{x_2h_1-x_1h_2}{h_2-h_1} - \tfrac{i\omega\kappa(x_2-x_1)}{g(h_2-h_1)} \quad \tilde{x}_3 = (x_2-x_1)/(h_2-h_1)\\ &\tilde{x}_4 = \tfrac{x_4h_2-x_3h_3}{h_3-h_2} - \tfrac{i\omega\kappa(x_4-x_3)}{g(h_3-h_2)} \quad \tilde{x}_5 = (x_4-x_3)/(h_3-h_2)\\ &\alpha_1(x) = \tfrac{2\omega}{\sqrt{g}}\sqrt{\tilde{x}_3}\sqrt{x+\tilde{x}_2} \qquad \alpha_2(x) = \tfrac{2\omega}{\sqrt{g}}\sqrt{\tilde{x}_5}\sqrt{x+\tilde{x}_4}\end{aligned} \tag{20}$$

B. General Solution of η and u

Now, we have 6 regions to determine the analytical solution of transmission and reflection coefficients, giving us 5 boundaries on which two corresponding solutions must match. To determine transmission and reflection coefficients, matching conditions need to be satisfied. The matching conditions are the continuity of the elevation and flux at each boundary point, x_i with $i = 0, 1, 2, 3, 4$. Below are the matching conditions for every x_i:

$$\overline{\eta}|_{x=x_i^-} = \overline{\eta}|_{x=x_i^+}, \qquad h\overline{u}|_{x=x_i^-} = h\overline{u}|_{x=x_i^+}. \tag{21}$$

From these conditions, we have two equations for every boundary (corresponding to the elevation and the flux), so that we will have 10 equations which can be written as a system of simultaneous equations:

$$\begin{aligned}-e^{-ik_0x_0}A_r + \zeta_0A_1 + \gamma_0A_2 &= e^{ik_0x_0}A_I,\\ ie^{-ik_0x_0}A_r + \sqrt{\tfrac{h_0}{g}}\tfrac{1}{\kappa_1\sqrt{\tilde{x}_1}}J_1(\beta_0)A_1 &\\ +\sqrt{\tfrac{h_0}{g}}\tfrac{1}{\kappa_1\sqrt{\tilde{x}_1}}Y_1(\beta_1))A_2 &= e^{ik_0x_0}A_I,\\ \zeta_1A_1 + \gamma_2A_2 - \zeta_2A_3 - \gamma_2A_4 &= 0,\\ \tfrac{1}{\sqrt{\tilde{x}_1}}(J_1(\beta_1)A_1 + Y_1(\beta_1)A_2) &\\ -\tfrac{1}{\sqrt{\tilde{x}_3}}(J_1(\beta_2)A_3 + Y_1(\beta_2)A_4) &= 0,\\ \zeta_3A_3 + \gamma_3A_4 - e^{ik_2x_2}A_5 - e^{-ik_2x_2}A_6 &= 0,\\ \tfrac{(h_2)^{\frac{3}{2}}}{(\kappa_2)^3\sqrt{g\tilde{x}_3}}J_1(\beta_3)A_3 + \tfrac{(h_2)^{\frac{3}{2}}}{(\kappa_2)^3\sqrt{g\tilde{x}_3}}Y_1(\beta_3)A_4 &\\ -e^{ik_2x_2}A_5 + e^{-ik_2x_2}A_6 &= 0,\\ e^{ik_2x_3}A_5 + e^{-ik_2x_3}A_6 - \zeta_4A_7 - \gamma_4A_8 &= 0,\\ e^{ik_2x_3}A_5 - e^{-ik_2x_3}A_6 - \tfrac{(h_2)^{\frac{3}{2}}}{(\kappa_3)^3\sqrt{g\tilde{x}_5}}J_1(\beta_4)A_7 &\\ -\tfrac{(h_2)^{\frac{3}{2}}}{(\kappa_3)^3\sqrt{g\tilde{x}_5}}Y_1(\beta_4)A_8 &= 0,\\ \zeta_5A_7 + \gamma_5A_8 &= e^{ik_3x_4}A_t,\\ \sqrt{\tfrac{h_3}{g}}\tfrac{1}{\kappa_4\sqrt{\tilde{x}_5}}J_1(\beta_5)A_7 + \sqrt{\tfrac{h_3}{g}}\tfrac{1}{\kappa_4\sqrt{\tilde{x}_5}}Y_1(\beta_5)A_8 &= e^{ik_3x_4}A_t,\end{aligned} \tag{22}$$

where

$$\begin{aligned}&\beta_0 = \tfrac{2\omega}{\sqrt{g}}\tilde{x}_1\kappa_1, \quad \beta_1 = \tfrac{2\omega}{\sqrt{g}}\tilde{x}_1\kappa_2, \quad \beta_2 = \tfrac{2\omega}{\sqrt{g}}\tilde{x}_3\kappa_2,\\ &\beta_3 = \tfrac{2\omega}{\sqrt{g}}\tilde{x}_3\kappa_3, \quad \beta_4 = \tfrac{2\omega}{\sqrt{g}}\tilde{x}_5\kappa_3, \quad \beta_5 = \tfrac{2\omega}{\sqrt{g}}\tilde{x}_5\kappa_4.\end{aligned} \tag{23}$$

$$\begin{aligned}\kappa_1 = \sqrt{h_0 - \tfrac{i\omega\kappa}{g}}, \quad \kappa_2 = \sqrt{h_1 - \tfrac{i\omega\kappa}{g}},\\ \kappa_3 = \sqrt{h_2 - \tfrac{i\omega\kappa}{g}}, \quad \kappa_4 = \sqrt{h_3 - \tfrac{i\omega\kappa}{g}},\end{aligned} \tag{24}$$

$$\begin{aligned}\zeta_0 &= \tfrac{1}{i\omega\left(\tilde{x}_1\kappa_1^2\right)^{\frac{3}{2}}}\left(-\tfrac{i\omega\kappa}{g}J_1(\beta_0) + \tfrac{\beta_0h_0}{2}J_0(\beta_0)\right),\\ \gamma_0 &= \tfrac{1}{i\omega\left(\tilde{x}_1\kappa_1^2\right)^{\frac{3}{2}}}\left(-\tfrac{i\omega\kappa}{g}Y_1(\beta_0) + \tfrac{\beta_0h_0}{2}Y_0(\beta_0)\right),\\ \zeta_1 &= \tfrac{1}{i\omega\left(\tilde{x}_1\kappa_2^2\right)^{\frac{3}{2}}}\left(-\tfrac{i\omega\kappa}{g}J_1(\beta_1) + \tfrac{\beta_1h_1}{2}J_0(\beta_1)\right),\\ \gamma_1 &= \tfrac{1}{i\omega\left(\tilde{x}_1\kappa_2^2\right)^{\frac{3}{2}}}\left(-\tfrac{i\omega\kappa}{g}Y_1(\beta_1) + \tfrac{\beta_1h_1}{2}J_0(\beta_1)\right),\\ \zeta_2 &= \tfrac{1}{i\omega\left(\tilde{x}_3\kappa_2^2\right)^{\frac{3}{2}}}\left(-\tfrac{i\omega\kappa}{g}J_1(\beta_2) + \tfrac{\beta_2h_2}{2}J_0(\beta_2)\right),\\ \gamma_2 &= \tfrac{1}{i\omega\left(\tilde{x}_3\kappa_2^2\right)^{\frac{3}{2}}}\left(-\tfrac{i\omega\kappa}{g}Y_1(\beta_2) + \tfrac{\beta_2h_1}{2}Y_0(\beta_2)\right),\\ \zeta_3 &= \tfrac{1}{i\omega\left(\tilde{x}_3\kappa_3^2\right)^{\frac{3}{2}}}\left(-\tfrac{i\omega\kappa}{g}J_1(\beta_3) + \tfrac{\beta_3h_2}{2}J_0(\beta_3)\right),\\ \gamma_3 &= \tfrac{1}{i\omega\left(\tilde{x}_3\kappa_3^2\right)^{\frac{3}{2}}}\left(-\tfrac{i\omega\kappa}{g}Y_1(\beta_3) + \tfrac{\beta_3h_2}{2}Y_0(\beta_3)\right),\\ \zeta_4 &= \tfrac{1}{i\omega\left(\tilde{x}_5\kappa_3^2\right)^{\frac{3}{2}}}\left(-\tfrac{i\omega\kappa}{g}J_1(\beta_4) + \tfrac{\beta_4h_2}{2}J_0(\beta_4)\right),\\ \gamma_4 &= \tfrac{1}{i\omega\left(\tilde{x}_5\kappa_3^2\right)^{\frac{3}{2}}}\left(-\tfrac{i\omega\kappa}{g}Y_1(\beta_4) + \tfrac{\beta_4h_2}{2}Y_0(\beta_4)\right),\\ \zeta_5 &= \tfrac{1}{i\omega\left(\tilde{x}_5\kappa_4^2\right)^{\frac{3}{2}}}\left(-\tfrac{i\omega\kappa}{g}J_1(\beta_5) + \tfrac{\beta_5h_3}{2}J_0(\beta_0)\right),\\ \gamma_5 &= \tfrac{1}{i\omega\left(\tilde{x}_5\kappa_4^2\right)^{\frac{3}{2}}}\left(-\tfrac{i\omega\kappa}{g}Y_1(\beta_5) + \tfrac{\beta_5h_5}{2}Y_0(\beta_5)\right).\end{aligned} \tag{25}$$

The equation system is then solved using the Elimination Method to obtain solutions for the unknown constants, which

are $A_r, A_1, A_2, A_3, A_4, A_5, A_6, A_7, A_8$ and A_t. The reflection and transmission coefficients are the ratios of the reflected amplitude (A_r) and transmitted amplitude (A_t) to the incoming wave amplitude (A_I), respectively. Consequently, we obtain the reflection coefficient (K_r) and the transmission coefficient (K_t) as follows.

$$K_r = \frac{\varphi_7\left(\gamma_0 - P\right) + \varphi_8\left(\zeta_0 - Q\right)}{2} e^{ik_0 x_0}, \tag{26}$$

$$K_t = \frac{2}{\varphi_7\left(\gamma_0 + P\right) + \varphi_8\left(\zeta_0 + Q\right)} e^{ik_0 x_0}. \tag{27}$$

where

$$\begin{aligned} P &= Y_1\left(\beta_0\right)\left(\frac{h_0}{\kappa_1^2}\right)^{\frac{3}{2}} \frac{1}{\sqrt{g\tilde{x}_1}}, \\ Q &= J_1\left(\beta_0\right)\left(\frac{h_0}{\kappa_1^2}\right)^{\frac{3}{2}} \frac{1}{\sqrt{g\tilde{x}_1}} \end{aligned} \tag{28}$$

The definition of the unknown variables φ_n, with n $1, 2, \ldots, 8$ are

$$\begin{aligned}
\varphi_8 = & \frac{\varphi_5\left(\gamma_2 Y_1(\beta_1) - \gamma_1 Y_1(\beta_2)\sqrt{\frac{\tilde{x}_1}{\tilde{x}_3}}\right)}{\zeta_1 Y_1(\beta_1) - \gamma_1 J_1(\beta_1)} \\
& + \frac{\varphi_6\left(\zeta_2 Y_1(\beta_1) - \gamma_1 Y_1(\beta_2)\sqrt{\frac{\tilde{x}_1}{\tilde{x}_3}}\right)}{\zeta_1 Y_1(\beta_1) - \gamma_1 J_1(\beta_1)}, \\
\varphi_7 = & \frac{\varphi_5\left(\gamma_2 J_1(\beta_1) - \zeta_1 Y_1(\beta_2)\sqrt{\frac{\tilde{x}_1}{\tilde{x}_3}}\right)}{\gamma_1 J_1(\beta_1) - \zeta_1 Y_1(\beta_1)} \\
& + \frac{\varphi_6\left(\zeta_2 J_1(\beta_1) - \zeta_1 J_1(\beta_2)\sqrt{\frac{\tilde{x}_1}{\tilde{x}_3}}\right)}{\gamma_1 J_1(\beta_1) - \zeta_1 Y_1(\beta_1)}, \\
\varphi_6 = & \frac{\varphi_4 e^{ik_2 x_3}\left(Y_1(\beta_3) - \gamma_3\left(\frac{\kappa_2^2}{h_2}\right)^{\frac{3}{2}}\sqrt{g\tilde{x}_3}\right)}{\zeta_3 Y_1(\beta_3) - \gamma_3 J_1(\beta_3)} \\
& + \frac{\varphi_3 e^{-ik_2 x_3}\left(Y_1(\beta_3) + \gamma_3\left(\frac{\kappa_3^2}{h_2}\right)^{\frac{3}{2}}\sqrt{g\tilde{x}_3}\right)}{\zeta_3 Y_1(\beta_3) - \gamma_3 J_1(\beta_3)}, \\
\varphi_5 = & \frac{\varphi_4 e^{ik_2 x_3}\left(J_1(\beta_3) - \zeta_3\left(\frac{\kappa_2^2}{h_2}\right)^{\frac{3}{2}}\sqrt{g\tilde{x}_3}\right)}{\gamma_3 J_1(\beta_3) - \zeta_3 Y_1(\beta_3)} \\
& + \frac{\varphi_3 e^{-ik_2 x_3}\left(J_1(\beta_3) + \zeta_3\left(\frac{\kappa_3^2}{h_2}\right)^{\frac{3}{2}}\sqrt{g\tilde{x}_3}\right)}{\gamma_3 J_1(\beta_3) - \zeta_3 Y_1(\beta_3)}, \\
\varphi_4 = & \frac{\varphi_1\left(\gamma_4 + Y_1(\beta_4)\left(\frac{h_2}{\kappa_3^2}\right)^{\frac{3}{2}}\frac{1}{\sqrt{g\tilde{x}_5}}\right)}{2} \\
& + \frac{\varphi_2\left(\zeta_4 + J_1(\beta_4)\left(\frac{h_2}{\kappa_3^2}\right)^{\frac{3}{2}}\frac{1}{\sqrt{g\tilde{x}_5}}\right)}{2} e^{-ik_2 x_3}, \\
\varphi_3 = & \frac{\varphi_1\left(\gamma_4 - Y_1(\beta_4)\left(\frac{h_2}{\kappa_3^2}\right)^{\frac{3}{2}}\frac{1}{\sqrt{g\tilde{x}_5}}\right)}{2} \\
& + \frac{\varphi_2\left(\zeta_4 - J_1(\beta_4)\left(\frac{h_2}{\kappa_3^2}\right)^{\frac{3}{2}}\frac{1}{\sqrt{g\tilde{x}_5}}\right)}{2} e^{ik_2 x_3}, \\
\varphi_2 = & \frac{Y_1(\beta_5) - \gamma_5\left(\frac{\kappa_4^2}{h_3}\right)^{\frac{3}{2}}\sqrt{g\tilde{x}_5}}{\zeta_5 Y_1(\beta_5) - \gamma_5 J_1(\beta_5)} e^{ik_3 x_4}, \\
\varphi_1 = & \frac{J_1(\beta_5) - \zeta_5\left(\frac{\kappa_4^2}{h_3}\right)^{\frac{3}{2}}\sqrt{g\tilde{x}_5}}{\gamma_5 J_1(\beta_5) - \zeta_5 Y_1(\beta_5)} e^{ik_3 x_4}.
\end{aligned} \tag{29}$$

IV. Results and Discussion

A. Hydrostatic Part

Here, we will discuss how our analytical solutions can be reduced into some well-known solutions, such as the analytical solution for a step with an infinite length [3] and a rectangular obstacle with a finite length [10].

1) Sloping Domain Ω_2, Ω_3 and Ω_5: To fit the case properly, we need to change some parameters of our model to convert the composite-sloped trapezoidal shape into a rectangular one. This may be achieved by setting $(x_1 - x_0) \rightarrow 0, (x_2 - x_1) \rightarrow 0$, and $(x_4 - x_3) \rightarrow 0$, hence $\beta_0 \rightarrow 0, \beta_1 \rightarrow 0, \beta_2 \rightarrow 0, \beta_3 \rightarrow 0, \beta_4 \rightarrow 0$, and $\beta_5 \rightarrow 0$. For these test cases, we will use $g = 9.81\ m/s^2$ as the acceleration due to gravity, $T = \pi/2\ s$ as the incoming wave period, and $A_i = 0.05\ m$ as the incoming wave amplitude. In this simulation, the diffusion coefficient is varied in the range of $0 \leq \kappa \leq 0.1$. The comparison between our analytical solutions (for various diffusion coefficient values) and solutions obtained in [10] is presented in Fig. 3.

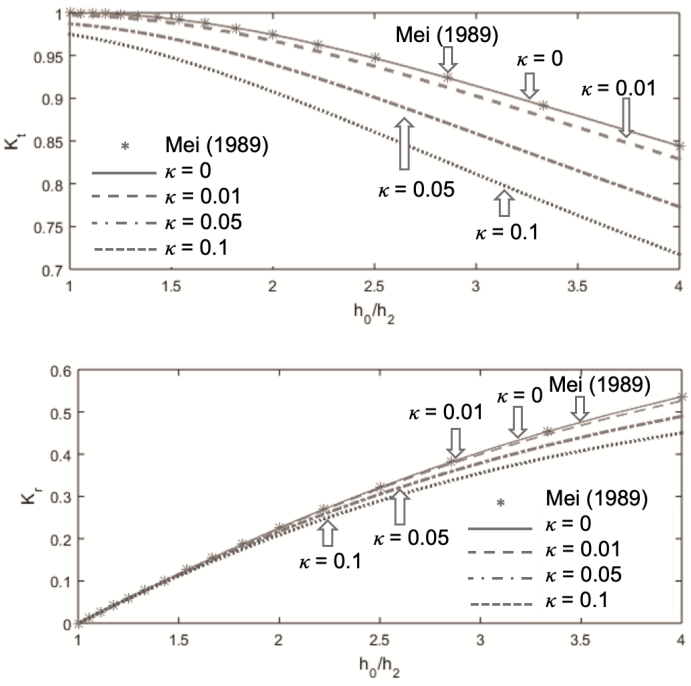

Fig. 3: Analytical solution K_t (upper) and K_r (lower) for rectangular breakwater case compared to solution obtained in [10] with $h_0 = h_1 = h_3 = 0.4\ m$, $0.1 \leq h_2 < 0.4$, and breakwater width $x_3 - x_2 = 0.25\ m$

Our analytical solution produces excellent agreement with the solution from [10]. Moreover, it may be seen that the transmission coefficient K_t never exceeds the value of 1. The solutions also show that as the height of the breakwater increases, $(h_2 \rightarrow 0)$, so the transmission coefficient decreases. Further, when diffusion coefficient is included, we can see that the transmission coefficient decreases as the diffusion coefficient increases. However, the reduction in K_t also depends on the height of the breakwater above the sea bed. In the limit, when $h_0 = h_2$ which means the waves propagate over a flat topography, the value of K_t is 1 for $\kappa = 0$. This is happen because in this condition, there will be no reflected waves and there is no diffusion effect that can decreases the amplitude. Notice that when we include the diffusion coefficient in the model, even in the flat bottom setting, the waves amplitude is still reduced. It might be

because in this model, we consider diffusion coefficient to exists in all domains except Ω_1 and Ω_6. Therefore, even when there is no breakwater, the diffusion remains in the domain and consequently reduce the waves amplitude.

As for the reflection coefficient, Fig. 3 shows that K_r decreases as the breakwater's height decreases. As the height of the breakwater tends to zero, so the value of K_r tends to zero because there will be no reflected wave in a flat bottomed basin. As for the reflection coefficient, the diffusion coefficient reduces K_r depending on the height ratio of the breakwater. Yet, the changes in diffusion coefficient give smaller changes in K_r than for K_t for the parameter ranges shown in Fig. 3.

The width of the breakwater crest is another important design parameter. To illustrate this, we consider the case where $h_0 = h_1 = h_3 = 0.4\ m$ and $h_2 = 0.15\ m$, while the width is changed within the range of $0.1 < (x_3 - x_2)/\lambda < 1.2$, where λ is the wave length. In this case, we vary the diffusion coefficient in the range of $0 \leq \kappa \leq 1$.

Solutions for the transmission and reflection coefficients in this case as a function of crest width are shown in Fig. 4. The solution presented in [10] is shown in blue asterisks and is extremely well matched by our solution, shown as the full red line. Further solutions for various values of diffusion coefficient are shown in broken and dashed lines. As we can see in Fig. 4, K_t and K_r vary periodically with the width of the breakwater. The introduction of diffusion dampens the oscillatory behaviour.

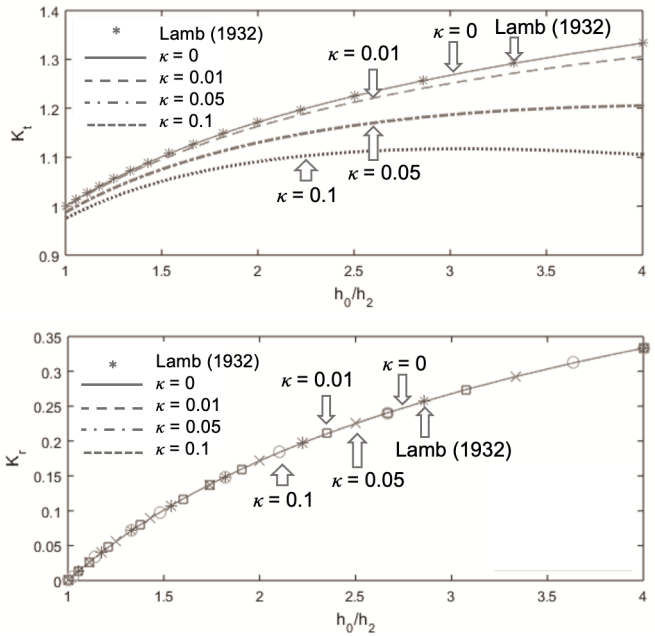

Fig. 4: Analytical K_t (upper) and K_r (lower) vs $M2$, where $M2 = (x_3 - x_2)/\lambda$, with λ is the wave length

2) Sloping Domain Ω_2, Ω_3 and Ω_5: A second 'canonical' problem has been selected to provide additional testing and illustration of our new solution. This is the propagation of a wave over a semi-infinite shelf. In this instance there are two cases: wave propagation from shallow to deep water with $h_0 = h_1 = h_2 < h_3$(left infinite step) and wave propagation from deep to shallow water with $h_3 = h_2 < h_0 = h_1$ (right infinite step). In this test case, we will only present the validation of our model for the right infinite step, to see how our model works on wave propagation to the shore and the shoaling phenomena. Below are the analytical results of K_t for various values of step height (or various values of h_2). We use the same parameters that have been used in rectangular test case which are $g = 9.81\ m/s^2$ as the gravity acceleration, $T = \pi/2$ s as the incoming wave period, and $A_i = 0.05\ m$ as the incoming wave amplitude. Fig. 5 shows the comparison between our model and the result given by [3] for the right infinite step case, as well as the effect of the changes in diffusion coefficient on wave transmission and reflection coefficient. The diffusion coefficient used in this simulation is in the range of $0 \leq \kappa \leq 0.1$.

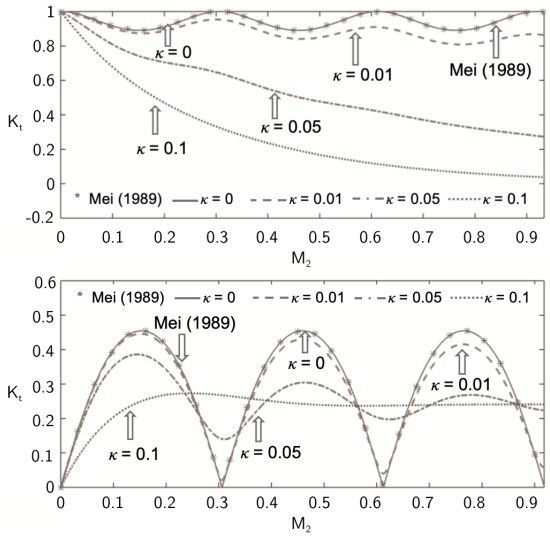

Fig. 5: Plot of K_t (upper) and K_r (lower) vs ratio of depth on top of the right infinite step and depth of flat bottom domain in front of it with $h_0 = 0.4\ m$

In addition to the results of the rectangular case, our model also gives a very good agreement with the theory given by [3]. Fig. 5 shows that for the case of a right infinite step, K_t increases as the step becomes closer to the water surface, and so does the value of K_r. We can see that when $h_2 = 0.1\ m$, the value of K_t is more than $1.3\ m$ which is larger than 1, and it is always more than or equal to one for any other value of h_2. It is caused by the phenomenon called shoaling, which makes wave amplitude increase when it propagates over a shallower domain and there is no other structure to hold it down. K_r rises because the higher the step, the more wave amplitude is reflected back to the ocean, causing A_r to rise and K_r to rise as well.

After κ is included, we can see the differences between the diffusion effects on K_t and K_r. In the case of K_t, as in the rectangular case, the effect of $kappa$ varies depending on the height ratio between the depth at the top of the step and the flat bottom depth. As the step becomes higher, the diffusion coefficient reduces the value of K_t more significantly. As the step becomes equal to the flat bottom, the diffusion coefficient can only be reduced slightly. The interesting result for K_r is that no matter how big the value of κ, there is no change in the value of K_r. This happens because, for infinite steps, we technically divided the domain into two domains, the deeper domain and the shallower domain. The reflected

waves only exist in the deeper domain caused by the waves that crash against the step, while in the shallower domain, the waves are all transmitted to the shore. Meanwhile, the diffusion coefficient is only included in the shallower domain, according to our initial assumptions. Hence, the diffusion coefficient will not affect the reflected amplitude no matter how large the value is. This is different from the results produced by the rectangular structure. Because in the rectangular case, the reflection waves also exist on top of the crest where the diffusion is also present. Therefore, the changes in κ will affect K_r in the rectangular case.

B. Effect of Breakwater Characteristics

In this section, we will investigate the effect of a composite-sloped trapezoidal breakwater on wave transmission amplitude. In terms of wave parameters, we continue to use the same values from the test cases: $g = 9.81\ m/s^2$, $T = \pi/2$ s, and $A_i = 0.05$ m. We have investigated the effect of the crest's width in the rectangular test case, and we also studied the relationship between the height ratio in both the rectangular and infinite step test cases. Because the slopes barely affect the transmission coefficient, or K_t [2], the effect of the crest's width and height ratio on the transmission coefficient in composite-sloped trapezoidal breakwaters will most likely be the same as its effect in rectangular breakwaters and infinite step cases. Consequently, here we will only study the effect of the depth of the flat bottom behind the structure (h_3). In order to do that, we set $h_0 = 0.4\ m,\ h_1 = 0.3\ m$, and $h_2 = 0.1\ m$. The crest's width is set to be $x_3 - x_2 = 0.25\ m$. The value of h_3 is in the $0.1 \leq h_3 \leq 0.4\ m$ range.The results for how h_3 affects K_t, as well as how the diffusion coefficient will affect K_t are shown in Fig. 6.

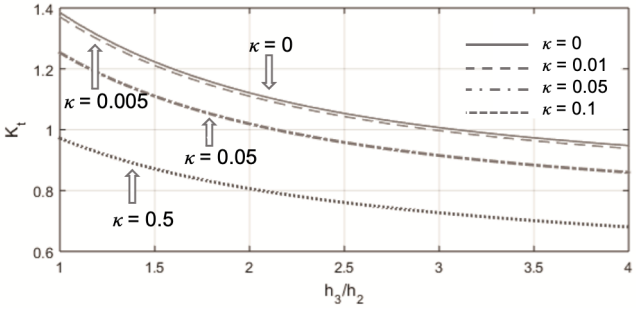

Fig. 6: Value of K_t depends on ratio h_3/h_2 with various value of κ

Fig. 6 shows us how h_3/h_2 affects the value of K_t. First, when the diffusion coefficient equals zero, the value of K_t decreases when the water depth behind the crest becomes deeper. The problem is, we can see that even with a backside depth of 0.4 m, which is as deep as the front bottom, the transmission coefficient is still high, which is equal to 0.9479. This is mostly because of the shoaling phenomena. The crest increases the wave amplitude significantly as the wave crashes against it, but the deeper bottom behind the crest is only enough to decrease the amplitude as much as it increases, maybe slightly bigger. However, in the actual phenomenon, we have considered the diffusion term caused by the breakwater itself. So now we will investigate how the diffusion helps the breakwater reduce the wave amplitude.

Fig. 6 also shows us that the diffusion term works nicely to reduce the transmission amplitude in the composite-sloped trapezoidal breakwater. We can see that as κ increases, the value of K_t decreases in all values of the ratio h_3/h_2. So, even if the breakwater itself is not enough to significantly decrease the wave amplitude, the diffusion effect caused by the breakwater will do it nicely. Even the small value of the diffusion coefficient can significantly reduce K_t. The effect of the diffusion coefficient on transmitted wave amplitude in general can be seen in Fig. 7.

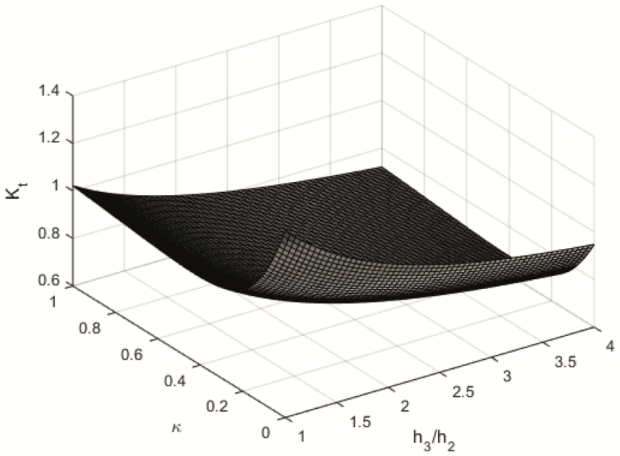

Fig. 7: Effect of diffusion coefficient κ on wave transmission coefficient K_t

Results from Fig. 7 show the transmission coefficient depends on the diffusion coefficient, κ produced by the analytical solution of our model. We still use the same set-up, where the depths are $h_0 = 0.4\ m,\ h_1 = 0.3\ m,\ h_2 = 0.1\ m$. The backside depth is in the range of $0.1 \leq h_3 \leq 0.4\ m$. From the figure, we can conclude that κ has successfully reduced the transmission coefficient smoothly. Again, the large value of κ is not necessary to reduce the amplitude. In fact, if we can use a small value of κ, then K_t will be reduced significantly. The figure also shows that, after a certain point, increasing the value of κ no longer significantly reduces the amplitude of the waves, and that the effect of diffusion remains the same for larger values of κ.

C. Composite-slope Trapezoidal Breakwater Application on Aceh's Bathymetry

Here, we will apply our analytical model to real topography, which is a cross-sectional bathymetry of the coast of Aceh, in Sumatra, Indonesia, where the 2014 tsunami occurred. This topography has been studied in order to better understand the shoaling phenomenon on such bathymetry [2]. The study results showed that the wave height on the shallower domain became more than two times bigger than the incoming waves on the deeper domain. This is why the tsunami waves that hit Aceh in 2004 are very dangerous. In this case, we will study what could happen if we placed a breakwater, especially a composite-slope trapezoidal breakwater, over the transmission region, where the amplitude

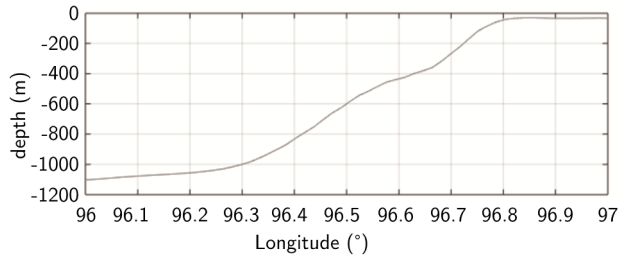

Fig. 8: Bathymetry of the coast of Aceh, Sumatera, Indonesia

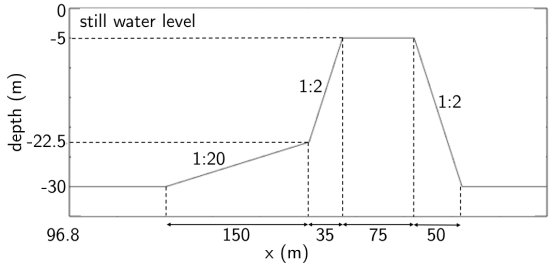

Fig. 9: Set-up of the composite-slope trapezoidal breakwater placed on top of the transmission region of Aceh's bathymetry

increases. We will see whether the breakwater can decrease the wave amplitude or not.

The real bathymetry is more complex and unsteady (see Fig. 8). Hence, to apply our linear model, we need to adjust a few things. First, we will only consider the transmission domain where the wave amplitude has already increased and place the breakwater on top of it. The transmission domain is defined by $x > 96.8$. Secondly, we transform the domain into a linearized topography so that we can apply our model. The transmission domain is approximated to be $30\ m$ deep. With that, we can place the breakwater over the transmission domain with a set-up as shown in Fig. 9.

We will investigate the transmitted amplitude of tsunami waves after they propagate over the breakwater using the setup depicted in Fig. 9. The incoming wave that we use in this case is the transmitted wave obtained by [2] with a wave height of $2.44\ m$ and a wave period of 17 minutes. For diffusion coefficient $\kappa = 0$, the transmitted coefficient obtained after the waves pass over the breakwater is 0.9975 which is less than 1. This means that the amplitude of the waves is successfully reduced by the breakwater, even though the diffusion has not been included. However, we also want to study how the diffusion affects the tsunami waves in this configuration. The value of K_t as a result of the changes of κ is presented in Fig. 10.

From Fig. 10, the most noticeable result is that we need a very large κ to slightly reduce the wave transmitted amplitude. This result is different from the previous result, where only a small value of κ can significantly reduce the wave amplitude. The most possible reason is because of the wave's characteristics itself. In this case, the incoming wave is a very long and big wave. So, it makes sense if we need a bigger κ to reduce the waves as significantly as the small κ reduces a small wave.

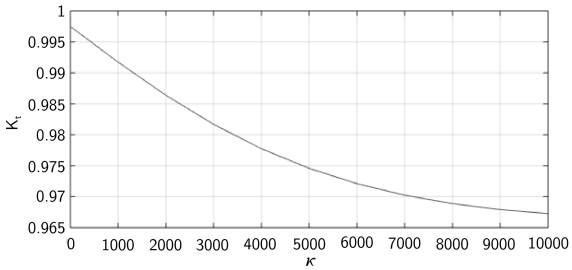

Fig. 10: Transmitted coefficient K_t for various value of κ for waves propagation over the Aceh's bathymetry

V. Conclusions

In this paper, we present new analytical solutions for wave propagation over a composite-sloped submerged trapezoidal breakwater in the form of wave transmission and reflection coefficients. These analytical solutions are then compared to other previously published solutions for simpler breakwater structures, such as rectangular breakwaters or infinite steps. In both cases, our analytical solutions and the previously well-known solutions agree very well. Furthermore, the effect of composite-sloped trapezoidal breakwater properties, as well as the diffusion coefficient, on wave height reduction has been studied. It was discovered that the deeper region behind the crest acts as a dissipator, reducing the amplitude induced by the shoaling phenomenon. However, this is insufficient to significantly reduce the wave amplitude. The turbulence effect, represented by the diffusion term, comes into play here to assist the breakwater in reducing the wave amplitude that propagates over it. And, as expected, as the diffusion coefficient increases, the wave transmission coefficient decreases, resulting in a reduction in wave amplitude. Finally, we used actual bathymetry from the coast of Aceh, Sumatera, Indonesia to investigate the effect of the breakwater on reducing tsunami wave amplitude. The results suggest that the breakwater can help minimise the amplitude of tsunami waves moderately, and to optimise that feature, the diffusion coefficient or turbulence effect can be adjusted to be as large as possible. It also reveals that the ability of the diffusion coefficient to minimise wave amplitude relies on the nature of the wave itself, with the coefficient being less powerful on long waves like tsunamis than it is on shorter waves.

References

[1] M. S. Longuet-Higgins and R. W. Stewart, "Radiation stresses in water waves; a physical discussion, with applications," *Deep-Sea Research and Oceanographic Abstracts*, vol. 11, no. 4, pp. 529–562, 1964.

[2] I. Magdalena, Iryanto, and D. E. Reeve, "Free-surface long wave propagation over linear and parabolic transition shelves," *Water Science and Engineering*, vol. 11, no. 4, pp. 318–327, 2018.

[3] H. Lamb, *Hydrodynamics*, 6th ed. Dover Publications, Inc., 1932.

[4] E. F. Bartholomeusz, "The reflection of long waves at a step," *Mathematical Proceedings of the Cambridge Philosophical Society*, vol. 54, no. 1, pp. 106–118, 1958.

[5] E. G. Bautista, E. Arcos, and O. E. Bautista, "Propagation of ocean waves over a shelf with linear transition," *Mecanica Computacional*, vol. 30, no. 4, pp. 225–242, 2011.

[6] M. R. Eldrup and T. L. Andersen, "Numerical study on regular wave shoaling, de-shoaling and decomposition of free/bound waves on gentle and steep foreshores," *Journal of Marine Science and Engineering*, vol. 8, no. 5, p. 334, 2020.

[7] J. Knowles and H. Yeh, "On shoaling of solitary waves," *Journal of Fluid Mechanics*, vol. 848, pp. 1073–1097, 2018.

[8] H. Jeffreys, "Motion of waves in shallow water: Note on the offshore bar problem and reflection from a bar," Great British Ministry of Supply, Tech. Rep., 1944.

[9] C. C. Mei and J. L. Black, "Scattering of surface wave by rectangular obstacles in waters of finite depth," *Journal of Fluid Mechanics*, vol. 38, no. 3, pp. 499–511, 1969.

[10] C. C. Mei, *The Applied Dynamics of Ocean Surface Waves*, 2nd ed. World Scientific, 1989.

[11] P. Lin, "A numerical study of solitary wave interaction with rectangular obstacles," *Coastal Engineering*, vol. 51, no. 1, pp. 35–51, 2004.

[12] F. S. Cao and B. Teng, "Analysis of wave passing a submerged breakwater by a scaled boundary finite element method," in *New Trends in Fluid Mechanics Research*, F. G. Zhuang and J. C. Li, Eds. Berlin: Springer, 2007.

[13] I. Magdalena, M. F. Atras, L. Sembiring, M. A. Nugroho, R. S. B. Labay, and M. P. Roque, "Wave transmission by rectangular submerged breakwaters," *Computation*, vol. 8, no. 2, p. 56, 2020.

[14] X. P. Yu and A. T. Chwang, "Wave motion through porous structures," *Journal of Engineering Mechanics*, vol. 120, no. 5, pp. 989–1008, 1994.

[15] A. N. Williams and K. H. Wang, "Flexible porous wave barrier for enchanced wetlands restoration," *Journal of Engineering Mechanics*, vol. 129, no. 1, pp. 1–8, 2003.

[16] I.-H. Cho, "Transmission coefficients of a floating rectangular breakwater with porous side plates," *International Journal of Naval Architecture and Ocean Engineering*, vol. 8, no. 1, pp. 53–65, 2016.

[17] M. M. Han and C. M. Wang, "Hydrodynamics study on rectangular porous breakwater with horizontal internal water channels," *Journal of Ocean Engineering and Marine Energy*, vol. 6, pp. 377–398, 2020.

[18] E. Masoudi and L. Gan, "Diffraction waves on large aspect ratio rectangular submerged breakwaters," *Ocean Engineering*, vol. 209, p. 107474, 2020.

[19] R. B. Kaligatla, N. M. Prasad, and S. Tabssum, "Oblique interaction between water waves and a partially submerged rectangular breakwater," *Journal of Engineering for The Maritime Environment*, vol. 234, no. 1, pp. 154–169, 2019.

[20] X. Zhang, Q. Zeng, and Z. Liu, "Hydrodynamic performance of rectangular heaving buoys for an integrated floating breakwater," *Journal of Marine Science and Engineering*, vol. 7, no. 8, p. 239, 2019.

[21] R. A. Dalrymple and J. Kirby, "Water waves over ripples," *Journal of Waterway Port Coastal and Ocean Engineering*, vol. 112, no. 2, pp. 309–319, 1986.

[22] P. Lin and H. W. Liu, "Analytical study of linear long-wave reflection by a two-dimensional obstacle of general trapezoidal shape," *Journal of Engineering Mechanics*, vol. 131, no. 8, pp. 822–830, 2005.

[23] H.-K. Chang and J.-C. Liou, "Long wave reflection from submerged trapezoidal breakwaters," *Ocean Engineering*, vol. 34, no. 1, pp. 185–191, 2007.

[24] H. Behera and M. B. M. Khan, "Numerical modeling for wave attenuation in double trapezoidal porous structures," *Ocean Engineering*, vol. 184, pp. 91–106, 2019.

[25] J. Chen, C. Jiang, S. Hu, and W. Huang, "Numerical study on the characteristics of flow field and wave propagation near submerged breakwater on slope," *Acta Oceanologica Sinica*, vol. 29, no. 1, pp. 88–99, 2010.

[26] V. Rey, M. Belzons, and E. Guazelli, "Propagation of surface gravity waves over a rectangular submerged bar," *Journal of Fluid Mechanics*, vol. 235, pp. 453–479, 1992.

[27] D. Stamos and M. R. Hajj, "Reflection and transmission of waves over submerged breakwaters," *Journal of Engineering Mechanics*, vol. 127, no. 2, pp. 99–105, 2001.

[28] S. M. Mahmoudof and F. Hajivaliea, "Experimental study of hydraulic response of smooth submerged breakwaters to irregular waves," *Oceanologia*, vol. 63, no. 4, pp. 448–462, 2021.

[29] Y. Chen, G. Niu, and Y. Ma, "Study on hydrodynamics of a new comb-type floating breakwater fixed on the water surface," *E3S Web of Conferences*, vol. 79, p. 02003, 2019.

[30] I. L. Neto, "Wave reflection from submerged rectangular obstacles: Experiments and predictive formula," *Acta Scientiarum. Technology*, vol. 40, no. 1, p. e37520, 2018.

[31] S. Beji and J. A. Battjes, "Experimental investigation of wave propagation over a bar," *Coastal Engineering*, vol. 19, no. 1-2, pp. 151–162, 1993.

[32] T. Ohyama, W. Kiota, and A. Tada, "Applicability of numerical models to nonlinear dispersive waves," *Coastal Engineering*, vol. 24, no. 3-4, pp. 297–313, 1994.

[33] N. Garcia, J. L. Lara, and I. J. Losada, "2-d numerical analysis of near-field flow at low-crested permeable breakwaters," *Coastal Engineering*, vol. 51, no. 10, pp. 991–1020, 2004.

[34] M. Kramer, B. Zanuttigh, J. W. van der Meer, C. Vidal, and F. X. Gironella, "Laboratory experiments on low-crested breakwaters," *Coastal Engineering*, vol. 52, no. 10-11, pp. 867–885, 2005.

[35] O. G. Nwogu, "Numerical prediction of breaking waves and currents with boussinesq model," *25th International Conference on Coastal Engineering*, pp. 4807–4820, 1997.

[36] J. Pedlosky, *Geophysical Fluid Dynamics*, 2nd ed. SpringerVerlag, 1987.

[37] B. Cushman-Roisin and J.-M. Beckers, *Introduction to Geophysical Fluid Dynamics*, 2nd ed. Academic Press, 1994.

[38] N. Jiang, W. Layton, M. McLaughlin, Y. Rong, and H. Zhao, "On the foundations of eddy viscosity models of turbulence," *Fluids*, vol. 5, no. 4, p. 167, 2020.